Evidence for Room Temperature Electric Polarization in $R\text{Mn}_2\text{O}_5$ Multiferroics

V. Balédent,[1] S. Chattopadhyay,[1] P. Fertey,[2] M. B. Lepetit,[3,4] M. Greenblatt,[5] B. Wanklyn,[6] F. O. Saouma,[7]
J. I. Jang,[7] and P. Foury-Leylekian[1]
[1]*Laboratoire de Physique des Solides, 91400 Orsay, France*
[2]*Synchrotron SOLEIL, L'Orme des Merisiers, BP 48 Saint-Aubin, 91192 Gif-sur-Yvette Cedex, France*
[3]*Institut Néel, 38042 Grenoble, France*
[4]*Institut Laue Langevin, 38000 Grenoble, France*
[5]*Department of Chemistry and Chemical Biology, Rutgers, the State University of New Jersey, Piscataway, New Jersey 08854, USA*
[6]*Clarendon Laboratory, Oxford University, Oxford OX1 3PU, England*
[7]*Department of Physics, Applied Physics and Astronomy, Binghamton University, P.O. Box 6000, Binghamton, New York 13902, USA*
(Received 12 November 2014; revised manuscript received 17 February 2015; published 16 March 2015)

It is established that the multiferroics $R\text{Mn}_2\text{O}_5$ crystallize in the centrosymmetric *Pbam* space group and that the magnetically induced electric polarization appearing at low temperature is accompanied by a symmetry breaking. However, both our present x-ray study—performed on compounds with $R = \text{Pr, Nd, Gd, Tb}$, and Dy—and first-principles calculations unambiguously rule out this picture. Based on structural refinements, geometry optimization, and physical arguments, we demonstrate in this Letter that the actual space group is likely to be *Pm*. This turns out to be of crucial importance for $R\text{Mn}_2\text{O}_5$ multiferroics since *Pm* is not centrosymmetric. Ferroelectricity is thus already present at room temperature, and its enhancement at low temperature is a spin-enhanced process. This result is also supported by direct observation of optical second harmonic generation. This fundamental result calls into question the actual theoretical approaches that describe the magnetoelectric coupling in this multiferroic family.

DOI: 10.1103/PhysRevLett.114.117601 PACS numbers: 77.84.−s, 61.05.cp, 77.80.−e

Interest in multiferroic materials is twofold: fundamental questions that are yet to be properly addressed and potential technological applications. Both of these aspects mainly originate from one common issue, i.e., the intrinsic coupling among the different order parameters. Magnetoelectric coupling is attracting major attention not only because it opens a wide range of applications in the field of emerging spintronic materials, but also because its microscopic mechanism requires exotic theories [1]. The strongest magnetoelectric effect is found in the so-called magnetically induced ferroelectrics, where the electric polarization appears at low temperature due to magnetic ordering. One of the archetypical systems is $R\text{MnO}_3$ (R is a the rare earth ion), for which the spin-induced ferroelectricity is theoretically ascribed to the Dzyaloshinskii-Moriya (DM) interaction (which mixes the structural and magnetic degrees of freedom [2]). This standard model describes the inversion symmetry breaking when a complex and noncollinear magnetic order (cycloidal, helicoidal, etc.) sets in. However, another family of manganites with general formula $R\text{Mn}_2\text{O}_5$ challenges the community because in these systems the ferroelectricity is induced by a quasicollinear magnetic order, thus ruling out the standard DM model [3]. This points to the primary importance of both magnetic and crystallographic structure determination to understand the microscopic mechanism breaking the centrosymmetry and leading to the electric polarization. It justifies the extensive studies performed on the different members of this family, especially for R from Tb to Tm [4–9]. According to the literature, all those compounds crystallize in the *Pbam* space group at room temperature and undergo a similar series of magnetic transitions at low temperature [10–12]. The electric polarization generally appears together with the incommensurate-to-commensurate magnetic-order transition (around 30 K, this temperature slightly depends on the rare earth). This behavior does not extend to lighter rare earth compositions such as PrMn_2O_5, which has been reported to be nonferroelectric [13]. Since the space group at room temperature (*Pbam*) is centrosymmetric, no electric polarization is possible, and its emergence at low temperature can only be ascribed to the quasicollinear spin ordering. From theoretical point of view, an exchange striction mechanism is often introduced to explain the spin-induced ferroelectricity [14]: the system tends to minimize the underlying magnetic frustration by slight atomic displacements leading to the breaking of the inversion symmetry and the electric polarization.

In this Letter, we report for the first time an exhaustive study of structural properties, as well as first-principles geometry optimizations, of the room temperature paramagnetic phase for the $R\text{Mn}_2\text{O}_5$ series. We rule out not only the *Pbam* space group, but we also find that the actual space group is noncentrosymmetric. This result calls into question the origin of the magnetoelectric coupling and the spin-induced exchange striction model. More importantly, it strongly suggests a preexisting electric polarization at room temperature.

Single crystals of a fraction of mm^3 for different members of the $R\mathrm{Mn_2O_5}$ series ($R = \mathrm{Pr, Nd, Gd, Tb}$ and Dy) were selected. These samples were synthesized either by flux method (small R size) or electrolysis (large R size). Details of the synthesis procedure are given in references [15,16]. We performed x-ray diffraction measurements with four-circle diffractometers, either at the SOLEIL synchrotron CRISTAL beam line (for $R = \mathrm{Tb, Gd}$, and Dy) or using the Mo$K\alpha$ radiation from laboratory sources (for $R = \mathrm{Pr}$ and Nd). The measurements were performed at room temperature for all compounds and at 100 K for $\mathrm{TbMn_2O_5}$.

In the $Pbam$ space group, $H0L$ and $0KL$ Bragg reflections are forbidden whenever H and K are odd. These forbidden reflections were however systematically observed for every measured compounds. Figure 1 displays reciprocal lattice reconstructions of the $0KL$ and $H0L$ planes for $\mathrm{DyMn_2O_5}$, in which the presence of the forbidden reflections is the most prominent. Before going any further, we checked for the possibilities of different experimental artifacts which could have been at the origins of these additional intensities. Neither a wavelength harmonic contamination ($\lambda/2$) nor the twinning of the crystal could explain the presence of such forbidden reflections. The possibility of a multiple scattering effect was also ruled out using an azimuthal scan [rotation of 10° with a step of 2° around the (007) reciprocal wave vector] since the intensity of the Bragg reflection was found to be nearly constant within the whole azimuthal range. The observed forbidden reflections thus cannot be associated with an experimental artifact, and since they are observed in the different members of the family, we can conclude that this superstructure is an intrinsic structural property of the $R\mathrm{Mn_2O_5}$ compounds at 300 K. It is important to notice that the presence of forbidden reflections was also observed in previous work, but without any reliable explanation of their origin [17]. We underline that all measured reflections present the experimental resolution while no diffuse scattering has been observed. This demonstrates the high quality of our crystals without significant disorder or other defects such as nanotwining. Despite their systematic observation, the intensity of the superstructure peaks is 0.2 to 1.5% stronger in the middle angle range than in the small angle region. This behavior can neither be related to thermal factor effects, nor to an order-disorder transition, but rather suggests a displacive origin. In such a case, the intensity of the forbidden reflections is expected to be proportional to the square of the atomic displacements from the mean $Pbam$ space group positions. The average intensity of the forbidden reflections yields the order of magnitude of the atomic displacements to be about 0.05 Å. These displacements are larger than the ones generally observed for structural transitions like the Peierls transitions in the blue bronze [18] or in the tetrathiafulvalene-tetracyanoquinodimethane (TTF-TCNQ) [19]. Table I shows the intensity ratios of the forbidden reflections compared to the allowed Bragg reflections for various compounds. It is noteworthy that this ratio does not seem to depend on the nature and on the size of the rare earth R atoms. Indeed, for the Nd, Gd, and Tb based compositions, the ratio is of the same order of magnitude. However, for Dy, it is 5 times greater than for the other members of the series. On the other hand, the mean intensity increase of

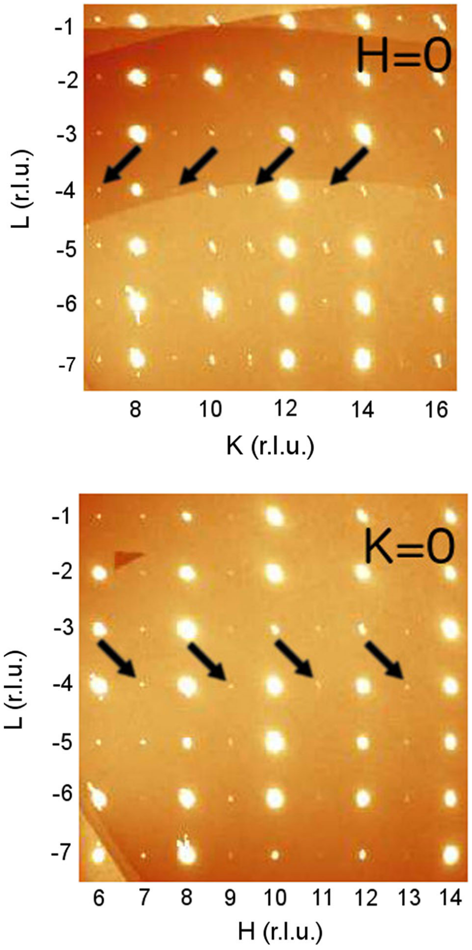

FIG. 1 (color online). Reconstructions of the lattice node planes $(0, K, L)$ (top) and $(H, 0, L)$ (bottom) of $\mathrm{DyMn_2O_5}$, taking into account absorption correction.

TABLE I. Critical temperature (T_{FE}), maximum electric polarization of various $R\mathrm{Mn_2O_5}$ compounds [20–22], and ratio between the mean integrated intensity of the forbidden reflections (I_S) and the mean integrated intensity of the allowed Bragg reflections (I_{Bragg}).

Sample	T_{FE} (K)	$(I_S/I_{\mathrm{Bragg}})(\%)$	Polarization ($\mu\mathrm{C \cdot m^{-2}}$)
$\mathrm{PrMn_2O_5}$		0.58	0
$\mathrm{NdMn_2O_5}$	25	0.27	3.5
$\mathrm{GdMn_2O_5}$	33	0.20	3600
$\mathrm{TbMn_2O_5}$	38	0.36	450
$\mathrm{DyMn_2O_5}$	39	1.40	200

the forbidden reflections destabilizes the ferroelectricity: the low temperature electric polarization is weaker in compounds where the ratio is stronger.

One can thus unambiguously assert that the actual space group cannot be *Pbam*. Among the orthorhombic space groups, only three are compatible with all the experimentally observed reflections, namely, *Pmmm*, *P*2*mm*, and *P*222. However, none of them are consistent with the mean *Pbam* structure. We therefore considered lower symmetry space groups. However, we are unable to detect a symmetry deviation from the orthorhombic cell parameters, the cell angles remaining 90° within a 0.1° accuracy. In the monoclinic setting, only three candidates are fully compatible with the observed Bragg reflections: $P2/m$, *P*2, and *Pm* (unique *c* axis). Lattice angles of 90° is unusual when considering monoclinic space groups. Nevertheless, a careful analysis of the reciprocal space reconstructions revealed minute deviations from 90°. Indeed, large segments instead of points are visible when the reciprocal space is projected along the *a* axis. This indicates that the γ angle is not exactly 90° but distributed around 90°, supporting the hypothesis of a monoclinic space group.

Among the three possible monoclinic space groups, a distinction has to be made between $P2/m$ on one hand, and *P*2 and *Pm* on another hand. Indeed, the former one is centrosymmetric while the latters are not. This question of centrosymmetry is the central issue regarding the ferroelectric properties of these materials, as glimpsed in the introduction.

Slight departure from the Friedel law should be observed thanks to the anomalous components of the atomic form factors, *f*'(*E*) and *f*"(*E*), for noncentrosymmetric groups [23]. Because of the strong absorption of $R\mathrm{Mn_2O_5}$ at the Mn *K* edge and rare earth *L* edge (both around 6 keV), anomalous scattering measurements at these edges is difficult. Therefore, we performed anomalous x-ray measurements on the $\mathrm{DyMn_2O_5}$ and $\mathrm{TbMn_2O_5}$ compounds just above the *K* edge energy of the rare earth atom (respectively, $53\,794 \pm 35$ eV and $52\,007 \pm 35$ eV). These compounds were chosen for their prominent forbidden reflections (see Table I). For both compounds, the differences between the intensities of the measured Friedel pairs were calculated. For the Dy compound, we observed that 1% of the 7000 measured Friedel pairs present a significant discrepancy above the 3 sigmas level. The average difference for these pairs was estimated to be 1%, with a maximum of 2% for the (2,0,0). Several reasons can explain this weak difference. i) In the absence of any external electric field, there exist twinned domains that may compensate the expected anomalous signal [23]. ii) When the resonant atom stays close to a centrosymmetric position, the corresponding *f*"(*E*) terms nearly compensate one another, weakening the intensity difference between the Friedel pair. Nevertheless, this non-negligible deviation of the Friedel law has to be taken into account and is in favor of a noncentrosymmetric structure.

Full data collection on $\mathrm{DyMn_2O_5}$ was performed at 28 keV, for structural determination (and at 21.4 keV for $\mathrm{TbMn_2O_5}$ and $\mathrm{GdMn_2O_5}$ compounds). Structure refinements were performed with the Jana software reference [24], considering the contributions of the different twins likely present in the samples (the introduction of twins only weakly improved the refinement and did nearly not modified the atomic positions). The anomalous scattering factors were taken from the Sasaki tables [25]. In the following, we will focus on the $\mathrm{DyMn_2O_5}$ data which were of the highest quality. Our refinements we were not able to distinguish among the different possible monoclinic structures. A joint refinement, using the data collected at 28 keV and at 53.8 keV, however shows slightly better *R* factors for *Pm* and *P*2 than for $P2/m$ and *Pbam* ($R = 3.32\%$, 3.41%, and 3.94% and 4.82%, respectively).

Simultaneously to these x-ray measurements, we performed density functional calculations in order to theoretically confirm the symmetry breaking. We optimized the $\mathrm{DyMn_2O_5}$ geometry in different subgroups of *Pbam*, using the CRYSTAL code [26,27]. We performed spin-polarized calculations using both ferromagnetic (FM) and antiferomagnetic (AFM) orders compatible with the *Pbam* space group. Let us note that since our calculations do not include spin orbit coupling, all magnetization axes are equivalent, and there is an AFM order similar to the one of Ref. [11] compatible with *Pbam*. In order not to be biased by the magnetic ordering (the high temperature phase is paramagnetic), we searched along line between the FM and AFM optimum geometries, the structure associated with the lowest average energy: $[E(\mathrm{FM}) + E(\mathrm{AFM})]/2$. In all cases, deviations from orthorhombic parameters remain very small ($< 0.01°$; see the Supplemental Material [27]). Our calculations easily ruled out the *Pbam* and $P2/m$ space groups. Indeed, the optimized *Pm* and *P*2 structures are about 500 meV per unit cell lower in energy than the *Pbam* one and 28 meV lower than the $P2/m$. The *P*2 optimized geometry is only 5 meV higher in energy than the *Pm* one. This energy difference is too small to be truly significant within a density functional theory scheme. Among the three possible monoclinic space groups, first principle calculations thus rule out the centrosymmetric group ($P2/m$). One can notice that the remaining *Pm* and *P*2 candidates are both polar groups [*Pm* with a polarization in the $(\boldsymbol{a}, \boldsymbol{b})$ plane and *P*2 in along the $\boldsymbol{c}$ axis].

The noncentrosymmetry was finally confirmed by the presence of optical second harmonic generation (see the Supplemental Material [27]). Together with the first principle calculations and the anomalous x-ray measurements, these results definitely rule out the centrosymmetric nature of the $R\mathrm{Mn_2O_5}$ systems at room temperature.

TABLE II. Atomic positions of $DyMn_2O_5$ at 300 K in the *Pm* space group ($R = 1.95\%$, $wR = 3.21\%$, $N = 28\,763$, $2\theta_{\min} = 1.47°$ $2\theta_{\max} = 41.44°$). The lattice parameters are $a = 7.2931$ Å, $b = 8.5025$ Å, and $c = 5.6743$ Å $\gamma = 90°$.

Atom	Site	x	y	z
$\mathrm{Dy1}_1$	1*a*	0.138 964(10)	0.171 696(7)	1
$\mathrm{Dy1}_2$	1*a*	−0.138 953(10)	−0.171 402(7)	−1
$\mathrm{Dy1}_3$	1*a*	0.638 754(10)	0.328 455(7)	−1
$\mathrm{Dy1}_4$	1*a*	−0.638 650(10)	−0.328 396(7)	1
$\mathrm{Mn1}_1$	2*c*	0.000 27(4)	0.499 93(3)	1.255 50(3)
$\mathrm{Mn1}_2$	2*c*	0.500 34(4)	0.000 17(3)	−1.255 49(3)
$\mathrm{Mn2}_1$	1*b*	0.411 62(4)	0.350 41(3)	0.5
$\mathrm{Mn2}_2$	1*b*	−0.411 97(4)	−0.350 02(3)	−0.5
$\mathrm{Mn2}_3$	1*b*	0.911 81(4)	0.149 42(3)	−0.5
$\mathrm{Mn2}_4$	1*b*	−0.911 91(4)	−0.150 32(3)	0.5
$\mathrm{O1}_1$	2*c*	0.0003(2)	−0.00065(15)	0.274 09(18)
$\mathrm{O1}_2$	2*c*	0.5002(2)	0.50265(14)	−0.270 48(16)
$\mathrm{O2}_1$	1*a*	0.162 90(15)	0.444 80(12)	0
$\mathrm{O2}_2$	1*a*	−0.1674(2)	−0.445 52(17)	0
$\mathrm{O2}_3$	1*a*	0.661 78(19)	0.055 94(13)	0
$\mathrm{O2}_4$	1*a*	−0.6592(2)	−0.05567(18)	0
$\mathrm{O3}_1$	1*b*	0.147 01(16)	0.419 71(14)	0.5
$\mathrm{O3}_2$	1*b*	−0.1514(2)	−0.433 36(14)	−0.5
$\mathrm{O3}_3$	1*b*	0.652 81(16)	0.062 49(13)	−0.5
$\mathrm{O3}_4$	1*b*	−0.6548(2)	−0.0612(2)	0.5
$\mathrm{O4}_1$	2*c*	0.395 43(17)	0.202 96(11)	0.253 33(19)
$\mathrm{O4}_2$	2*c*	−0.401 23(12)	−0.209 60(9)	−0.237 19(15)
$\mathrm{O4}_3$	2*c*	0.895 95(17)	0.293 07(11)	−0.2425(2)
$\mathrm{O4}_4$	2*c*	−0.891 74(13)	−0.295 66(10)	0.246 29(14)

Unfortunately, neither our refinements nor our calculations can distinguish *Pm* from *P*2 with enough confidence, even if in both cases the *Pm* group is favored. The structure of $DyMn_2O_5$ for the *Pm* space group obtained from the 28 keV high resolution data set is presented in Table II (*P*2 experimental structure as well as *Pm* and *P*2 theoretical ones can be found in the Supplemental Material [27]). The atomic deviations from the *Pbam* structure of Ref. [37] is analyzed in the following. As expected, a small deviation of the rare earth from its centrosymmetric position is observed (0.1 ± 0.02 pm). In fact, for both structures, the main atomic displacement concerns the oxygens labeled O3 and to a less extent the oxygens O4, respectively, located at the 4*h* and 8*i* Wyckoff positions in the *Pbam* space group. Their displacements ($\sim 7 \pm 1$ pm for O3 and $\sim 5 \pm 1$ pm for O4) are 1 or 2 orders of magnitude larger than the rare earth one. The Mn^{4+} ions are also slightly displaced (0.5 ± 0.05 pm). Naturally, the direction of the atomic displacements totally differs in the *P*2 and the *Pm* space groups. The same kind of displacements have been observed for $TbMn_2O_5$ and to a lesser extent (because of poorer quality data) for $GdMn_2O_5$. The role of the oxygen atoms in the deviation from the mean *Pbam* structure explains the lack of accuracy and statistics using x-ray scattering, as well as the difficulty to discriminate between the *Pm* and *P*2 space groups. The prominent role of the O3 (O4) oxygens in the deviation from the *Pbam* structure may have a strong impact in the multiferroic properties. Indeed, these oxygens are located between the Mn^{3+} and Mn^{4+} magnetic sites. Thus, they actively participate in the superexchange interactions J_4 (O3) and J_3 (O4) [10]. Consequently, any change in the oxygens positions largely influences the values of J_4 and J_3. As the superstructure magnitude is nearly 4 times stronger in $DyMn_2O_5$ than in $TbMn_2O_5$, J_4 and J_3 should significantly differ between these two compounds. Due to the presence of magnetic frustration, the magnetic order at low temperature is expected to be particularly sensitive to any variation of the J_i couplings. In light of these considerations, it appears natural that $DyMn_2O_5$ and $TbMn_2O_5$ exhibit completely different magnetic orders [11].

Despite the lack of experimental and theoretical accuracy to discern *P*2 from *Pm*, we can present other physical arguments in favor of the *Pm* symmetry. When a polarization is observed [20–22], it systematically points along the *b* axis (compatible with the *Pm* group, but not with the *P*2 one). It is likely that the high temperature symmetry is compatible with the symmetry of the low temperature polarization. There is however a subtlety in $TmMn_2O_5$ as it presents a polarization flip from the b to the a direction at low temperature [38]. Nevertheless, this flip is still compatible with *Pm*, but not with *P*2 (where $\vec{P}$ is along the ***c*** axis). These considerations therefore definitely preclude the *P*2 space group.

In conclusion, our study reveals that the universal space group of the RMn_2O_5 series at ambient temperature is not the expected *Pbam*, but the noncentrosymmetric *Pm* space group. The direct consequence of the noncentrosymmetric symmetry is the presence of electric polarization above the Néel temperature and even at room temperature. This fundamental result calls into question all theoretical approaches that deal with the origin of the magnetoelectric coupling in this multiferroic family. In addition, it gives a comprehensive understanding of the difference of magnetic orders among different members of the RMn_2O_5 series. Finally, since the inversion symmetry is already broken at room temperature, it is obvious that the magnetoelectric coupling in the RMn_2O_5 originates from a spin-enhanced process rather than from the spin-induced effect.

We thank T. Emge, A. Goukassov, and R. Guillot for their technical and scientific help. This work is supported by a public grant from the Laboratoire d'Excellence Physics Atom Light Mater (LabEx PALM) overseen by the French National Research Agency (ANR) as part of the Investissements d'Avenir Program No. ANR-10-LABX-0039, and by the IDRIS and CRIHAN computer centers under Projects No. ni2014081842 and No. n2007013. Support for M. G. was provided by DOD Grant No. W911NF-12-1-0172.

[1] S.-W. Cheong and M. Mostovoy, Nat. Mater. **6**, 13 (2007).

[2] I. A. Sergienko and E. Dagotto, Phys. Rev. B **73**, 094434 (2006).

[3] Y. Noda, H. Kimura, M. Fukunaga, S. Kobayashi, I. Kagomiya, and K. Kohn, J. Phys. Condens. Matter **20**, 434206 (2008).

[4] J. Koo, S. Ji, T. Jang, and Y. Jeong, J. Korean Phys. Soc. **51**, 562 (2007).

[5] C. Wang, G.-C. Guo, and L. He, Phys. Rev. Lett. **99**, 177202 (2007).

[6] Y. Noda, H. Kimura, and Y. Kamada, J. Korean Phys. Soc. **51**, 828 (2007).

[7] S. C. Abrahams, J. Chem. Phys. **46**, 3776 (1967).

[8] W. Ratcliff, V. Kiryukhin, M. Kenzelmann, S.-H. Lee, R. Erwin, J. Schefer, N. Hur, S. Park, and S.-W. Cheong, Phys. Rev. B **72**, 060407 (2005).

[9] C. R. dela Cruz, F. Yen, B. Lorenz, M. M. Gospodinov, C. W. Chu, W. Ratcliff, J. W. Lynn, S. Park, and S.-W. Cheong, Phys. Rev. B **73**, 100406 (2006).

[10] P. Radaelli and L. Chapon, J. Phys. Condens. Matter **20**, 434213 (2008).

[11] G. R. Blake, L. C. Chapon, P. G. Radaelli, S. Park, N. Hur, S.-W. Cheong, and J. Rodriguez-Carvajal, Phys. Rev. B **71**, 214402 (2005).

[12] C. Doubrovsky, G. André, F. Bouquet, E. Elkaim, M. Li, M. Greenblatt, and P. Foury-Leylekian, Physica (Amsterdam) **B407**, 1718 (2012).

[13] C. Doubrovsky, G. André, A. Gukasov, P. Auban-Senzier, C. R. Pasquier, E. Elkaim, M. Li, M. Greenblatt, F. Damay, and P. Foury-Leylekian, Phys. Rev. B **86**, 174417 (2012).

[14] J. van den Brink and D. I. Khomskii, J. Phys. Condens. Matter **20**, 434217 (2008).

[15] G. Popov, M. Greenblatt, and W. McCarroll, Mater. Res. Bull. **35**, 1661 (2000).

[16] B. Wanklyn, J. Mater. Sci. **7**, 813 (1972).

[17] J. Koo, C. Song, S. Ji, J. S. Lee, J. Park, T. H. Jang, C.-H. Yang, J.-H. Park, Y. H. Jeong, K. B. Lee, T. Y. Koo, Y. J. Park, J.-Y. Kim, D. Wermeille, A. I. Goldman, G. Srajer, S. Park, and S.-W. Cheong, Phys. Rev. Lett. **99**, 197601 (2007).

[18] W. J. Schutte and J. L. De Boer, Acta Crystallogr. Sect. B **49**, 579 (1993).

[19] Y. Bouveret and S. Megtert, J. Phys. (Paris) **50**, 1649 (1989).

[20] Z. Zhao, M. F. Liu, X. Li, L. Lin, Z. B. Yan, S. Dong, and J. Liu, Sci. Rep. **4**, 3984 (2014).

[21] S. Chattopadhyay, V. Balédent, F. Damay, A. Goukassov, E. Moshopolou, P. Auban-Senzier, C. Pasquier, G. André, F. Porcher, E. Elkaim, C. Doubrovsky, M. Greenblatt, and P. Foury-Leylekian (to be published).

[22] I. Kagomiya, K. Kohn, and T. Uchiyama, Ferroelectrics **280**, 131 (2011).

[23] C. Azimonte, E. Granado, H. Terashita, S. Park, and S. Cheong, Phys. Rev. B **81**, 012103 (2010).

[24] V. Petricek, M. Dusek, and L. Palatinus, Z. Kristallogr. **229**, 345 (2014).

[25] S. Sasaki, "Numerical Tables of Anomalous Scattering Factors Calculated by the Cromer and Liberman's Method," http://www.iaea.org/inis/collection/NCLCollectionStore/_Public/20/081/20081580.pdf.

[26] R. Dovesi, R. Orlando, A. Erba, C. M. Zicovich-Wilson, B. Civalleri, S. Casassa, L. Maschio, M. Ferrabone, M. De La Pierre, P. D'Arco, Y. Noel, M. Causa, M. Rerat, and B. Kirtman, Int. J. Quantum Chem. **114**, 1287 (2014).

[27] See Supplemental Material at http://link.aps.org/supplemental/10.1103/PhysRevLett.114.117601, which includes Refs. [28–36], for details on the structure refinement and calculations.

[28] R. J. Elliott, Phys. Rev. **124**, 340 (1961).

[29] A. S. Moskvin and R. V. Pisarev, Phys. Rev. B **77**, 060102 (2008).

[30] J. Jang, S. Park, D. Clark, F. Saouma, D. Lombardo, C. Harrison, and B. Shim, J. Opt. Soc. Am. **30**, 2292 (2013).

[31] J. Jang, A. Haynes, F. Saouma, C. Otieno, and M. Kanatzidis, Opt. Mater. Express **3**, 1302 (2013).

[32] R. Boyd, *Nonlinear Optics*, 3rd ed. (Academic Press, New York, 2008).

[33] S. Mani, J. Jang, and J. Ketterson, Opt. Lett. **34**, 2817 (2009).

[34] M. Peintinger, D. Vilela Oliveira, and T. Bredow, J. Comput. Chem. **34**, 451 (2013).

[35] M. Dolg, H. Stoll, A. Savin, and H. Preuss, Theor. Chim. Acta **75**, 173 (1989).

[36] J. P. Perdew, A. Ruzsinszky, G. I. Csonka, O. A. Vydrov, G. E. Scuseria, L. A. Constantin, X. Zhou, and K. Burke, Phys. Rev. Lett. **100**, 136406 (2008).

[37] S. Abrahams and J. Bernstein, J. Chem. Phys. **46**, 3776 (1967).

[38] M. Fukunaga, K. Nishihata, H. Kimura, Y. Noda, and K. Kohn, J. Phys. Soc. Jpn. **77**, 094711 (2008).